Am J Cancer Res 2022;12(9):4326-4342
www.ajcr.us /ISSN:2156-6976/ajcr0145663

Original Article

A novel DDR1 inhibitor enhances the anticancer activity of gemcitabine in pancreatic cancer

Soyeon Ko[1*], Kyung Hee Jung[1*], Young-Chan Yoon[1], Beom Seok Han[1], Min Seok Park[1], Yun Ji Lee[1], Sang Eun Kim[1], Ye Jin Cho[1], Pureunchowon Lee[1], Joo Han Lim[1], Ji-Kan Ryu[1], Kewon Kim[2], Tae Young Kim[3], Sungwoo Hong[2], So Ha Lee[3], Soon-Sun Hong[1]

[1]Department of Medicine, College of Medicine, and Program in Biomedical Science & Engineering, Inha University, 3-ga, Sinheung-dong, Jung-gu, Incheon 22332, Korea; [2]Center for Catalytic Hydrocarbon Functionalization, Institute of Basic Science (IBS) and Department of Chemistry, Korea Advanced Institute of Science and Technology (KAIST), Daejeon 34141, Korea; [3]Chemical Kinomics Research Center, Korea Institute of Science and Technology, Seoul 02792, Korea. [*]Equal contributors.

Received July 31, 2022; Accepted September 4, 2022; Epub September 15, 2022; Published September 30, 2022

Abstract: Pancreatic ductal adenocarcinoma (PDAC) is an extracellular matrix (ECM)-rich carcinoma, which promotes chemoresistance by inhibiting drug diffusion into the tumor. Discoidin domain receptor 1 (DDR1) increases tumor progression and drug resistance by binding to collagen, a major component of tumor ECM. Therefore, DDR1 inhibition may be helpful in cancer therapeutics by increasing drug delivery efficiency and improving drug sensitivity. In this study, we developed a novel DDR1 inhibitor, KI-301690 and investigated whether it could improve the anticancer activity of gemcitabine, a cytotoxic agent widely used for the treatment of pancreatic cancer. KI-301690 synergized with gemcitabine to suppress the growth of pancreatic cancer cells. Importantly, its combination significantly attenuated the expression of major tumor ECM components including collagen, fibronectin, and vimentin compared to gemcitabine alone. Additionally, this combination effectively decreased mitochondrial membrane potential (MMP), thereby inducing apoptosis. Further, the combination synergistically inhibited cell migration and invasion. The enhanced anticancer efficacy of the co-treatment could be explained by the inhibition of DDR1/PYK2/FAK signaling, which significantly reduced tumor growth in a pancreatic xenograft model. Our results demonstrate that KI-301690 can inhibit aberrant ECM expression by DDR1/PYK2/FAK signaling pathway blockade and attenuation of ECM-induced chemoresistance observed in desmoplastic pancreatic tumors, resulting in enhanced antitumor effect through effective induction of gemcitabine apoptosis.

Keywords: DDR1, pancreatic cancer, ECM, collagen, gemcitabine

Introduction

Pancreatic ductal adenocarcinoma (PDAC) is the most common form of pancreatic cancer, accounting for approximately 90% of all pancreatic tumors. PDAC is a devastating human malignancy, with an overall 5-year survival rate of less than 10% and a poor prognosis. Patients with PDAC have few opportunities to undergo surgery, resulting in poor prognosis and limited treatment options [1, 2]. Consequently, the only available treatment for advanced PDAC is chemotherapy, which often combines gemcitabine with other chemo-agents [3, 4]. However, these chemotherapeutics have shown high toxicity and low therapeutic efficacy. Additionally, clinically beneficial responses to gemcitabine are observed at approximately 10-20%. This limited therapeutic efficacy is associated with 3-6 months of overall survival due to acquired resistance [5, 6]. The clinical response failure can be attributed to poor drug penetration into dense tumor stroma with abundant extracellular matrix (ECM), and subsequent development of gemcitabine chemoresistance [7]. Therefore, a new strategy is required to improve the therapeutic efficacy of gemcitabine for the treatment of ECM-rich pancreatic cancer.

Tumors are affected by numerous stromal components including ECM, which enhance tumor phenotypes and therapy resistance [8]. ECM provides both biochemical and biomechanical cues, which are required for tumor progression

through activated cell signaling [9]. Among the proteins interacting with ECM, discoidin domain receptor 1 (DDR1) is the most prominently related to tumor progression and drug resistance. It belongs to a subfamily of receptor tyrosine kinases (RTKs) characterized by an extracellular discoidin homology domain to modulate cell proliferation and differentiation by interacting with several types of collagens [10]. Namely, DDR1 functions as an ECM signal transducer, binding to ECM collagen, and initiating intra-cellular signaling [11]. In different human cancers such as breast, esophageal, prostate, hepatocellular, lung, and pancreatic cancers, DDR1 has been implicated in tumor development and cancer progression [12-16]. A high expression of DDR1 in PDAC is correlated with poor prognosis. Additionally, DDR1 promotes local invasion and colonization of lung cancer, indicating its involvement in the metastatic niche [17]. Its expression has been reported to reduce sensitivity to chemotherapy, which may lead to cancer recurrence [18-20]. Recent studies have reported that increased DDR1 expression conferred chemoresistance to ovarian and lung cancers [21, 22]. This evidence shows that the targeting of DDR1 inhibits tumor growth, increases chemosensitivity, and improves acquired resistance in cancer therapeutics. Therefore, in this study, we developed a novel DDR1 inhibitor, KI-301690, and investigated its efficacy on gemcitabine co-treatment and its mechanism of action, *in vitro* and *in vivo.*

Materials and methods

Synthesis of KI-301690, a novel DDR1 inhibitor

The reaction of 2,4-dichloro-5-nitropyrimidine (1) with (2-nitrophenyl) methylamine resulted in chloropyrimidine (2) under base, followed by nucleophilic substitution reaction and reduction to produce a compound (3). KI-301690 was finally synthesized by the coupling of diamine (3) using carbonylimidazole, to produce an overall yield of 34%.

Tissue microarray

Normal human (n = 20) and pancreatic cancer (n = 80) tissue microarrays (US Biomax, Inc., Rockville, MD, USA) were used to examine p-DDR1 expression. Protein expression (high or low) in pancreatic cancer tissues was scored semi-quantitatively.

Cell culture

Human pancreatic cancer cell lines PANC-1, MIA PaCa-2, AsPC-1, HPAC, and Capan-2, and the normal pancreatic cancer cell HPNE were purchased from the American Type Culture Collection (ATCC, Manassas, VA, USA). They were cultured in Dulbecco's Modified Eagle's Medium (DMEM; Welgene, Gyeongsan, Korea) or Roswell Park Memorial Institute-1640 medium (RPMI-1640, Gibco, Waltham, MA, USA) supplemented with 10% fetal bovine serum (FBS, Gibco, Waltham, MA, USA) and 1% penicillin-streptomycin (Gibco, Waltham, MA, USA). All authenticated and mycoplasma free cell lines were maintained at 37°C in a CO_2 incubator with a controlled humidified atmosphere composed of 95% air and 5% CO_2.

MTT assay

The cell growth rate after the treatment of gemcitabine and/or KI-301690 was determined using a 3-(4,5-dimethylthiazol-2-yl)-2,5-diphenyl tetrazolium bromide (MTT) assay. The cells (PANC-1, 3000 cells; MIA PaCa-2, 2000 cells per well) were seeded in 96-well plates and treated for 72 h with different concentrations of KI-301690 and/or gemcitabine. Thereafter, 20 μL of a MTT solution (2 mg/mL) was added to each well, and the plate was incubated for another 4 h at 37°C. Then, the MTT containing culture medium was replaced with dimethyl sulfoxide (100 μL/well) and the plate was shaken to dissolve blue formazan crystals, whose absorbance was read at 540 nm by a microplate reader. The median inhibitory concentration for cell growth (IC_{50}, the drug concentration at which cell growth was inhibited by 50%) was assessed from dose-response curves.

Western blotting

Cells were lysed using a urea buffer and sonicated. The total protein content was estimated using the bicinchoninic acid (BCA) assay method, and an equivalent amount of protein was separated on sodium dodecyl sulfate polyacrylamide electrophoresis gel and transferred to a polyvinylidene difluoride (PVDF) membrane (Millipore, Bedford, MA, USA). The protein transfer was reviewed using Ponceau S solution staining (Biosesang, PR2059-050-00, Korea).

The membranes were blocked with phosphate-buffered saline (PBS) containing 5% skim milk at room temperature for 1 h and incubated overnight at 4°C with anti-DDR1 (Santa Cruz Biotechnology, 374618), anti-phospho DDR1 (Cell Signaling Technology, 11994), anti-phospho PYK2 (Invitrogen, 44-618G), anti-phospho FAK (Invitrogen, 700255), anti-Collagen I (Abcam, 34710), and anti-GAPDH (Santa Cruz Biotechnology, 25778) antibodies. Followed by washing with PBST three times, the membrane was incubated with either secondary antibody for 1 h. The secondary antibodies were diluted to 1:2000 in 4% skim milk. The proteins were visualized using Clarity™ Western ECL Substrate (Amer-sham Biosciences, Piscataway, NJ, USA). Protein expression was quantified by measuring the pixel intensity of each band using ImageJ software.

Immunocytochemistry

For immunofluorescence and image analysis, cells were seeded on coverslips and fixed in acetic acid:ethanol solution (1:2) for 10 min at 4°C. Fixed cells were permeabilized with 0.5% Triton X-100 for 10 min and incubated in CAS block solution (Life technologies) for 1 h at room temperature. Next, cells were incubated overnight at 4°C with a primary antibody: anti-phospho DDR1, anti-phospho PYK2, anti-phospho FAK, Collagen I (Genetex, GTX26308), Cleaved caspase 3 (Cell Signaling Technology, 9661), Vimentin (Sigma-Aldrich, V2258), Fibronectin (Abcam, 23750), and α-SMA (Sigma-Aldrich, F3777). After washing several times with PBS, cells were incubated with fluorescently labeled secondary antibodies (1:60) for 1 h and incubated for another 1 h at room temperature in a 1:100 dilution of 4,6-diamidino-2-phenylindole (DAPI) to visualize nuclei. They were viewed with a confocal laser-scanning microscope (Olympus) at wavelengths 488 and 568 nm.

Two chamber migration and invasion assay

To measure cell activity, transwell assays were performed using a 12-well plate with 8.0 μm transparent PET membrane (Corning, Corning, NY, USA). Additionally, the upper surface of the filter was coated with 10% matrigel (Corning, Corning, NY, USA) for 4 h. Cells suspended in serum-free DMEM and drug-treatment media were added to the upper chamber and lower chambers, respectively. After 72 h, migrated or invaded cells of the lower side of the inserts were fixed with 4% PFA and stained with 0.5% crystal violet. The purple region was quantified using ImageJ software.

Fluid shear stress assay

PANC-1 cells were treated for 72 h with different concentrations of KI-301690 and/or gemcitabine. Then, cells were trypsinized and resuspended to a concentration of 1×10^6 mL in culture medium and subjected to five repeated exposures to shear stress through a 30-gauge needle, followed by the application of a constant flow of 100 μL/s. Next, 2×10^3 cells were cultured in 96-well Ultra Low Cluster Round bottom plates (Costar) or 96-well flat bottom plates (FALCON) and incubated at 37°C. The size and shape of the 3D spheroids were recorded using an inverted light microscope from day 2 to day 11.

Measurement of mitochondrial transmembrane potential

The mitochondrial membrane potential (MMP) was detected using a JC-1 Mitochondrial Membrane Potential Assay Kit (Cayman Chemical, Ann Arbor, MI, USA). Cells (PANC-1, 8×10^4/well) were seeded on 18-mm coverslips and grown to approximately 70% confluence for 24 h. After attachment, the cells were treated with gemcitabine and/or KI-301690. Then, the culture medium of each well was replaced with JC-1 (Cayman Chemical, Ann Arbor, MI, USA) in PBS for 1 h at 37°C and fixed with 4% PFA for 5 min at room temperature. Next, cells were stained with DAPI for 1 h and slides were covered with Fluorescence Mounting Medium (Dako). They were visualized with a confocal laser scanning microscope (Olympus, Tokyo, Japan). For MitoTracker staining, cells were treated for 10 h and incubated with 200 nM MitoTracker Deep red FM (Invitrogen) at 37°C for 30 min. After removal of the media from the well, cells were fixed with a 4% PFA solution for 15 min at 37°C, and permeabilized with 0.5% Triton X-100 for 3 min at room temperature. Then, the cells were incubated in CAS block solution (Life Technologies) for 40 min at room temperature and incubated over night at 4°C with cytochrome C antibody (Santa Cruz Biotechnology, 13156). Fluorescently labeled secondary antibodies (1:60) were incubated for 1 h

and stained with DAPI diluted 1:100 in PBS. Finally, slides were covered with Fluorescence Mounting Medium (Dako) and visualized using a confocal laser scanning microscope (Olympus, Tokyo, Japan).

Terminal deoxynucleotidyl transferase (TdT) dUTP nick-end labeling (TUNEL) assay

Cells were briefly seeded onto 18-mm coverslips and fixed with acetic acid and ethanol solution, also using 3-μm-thick sections of the tumor samples after deparaffinization. Fixed cells and tissue were permeabilized with 0.5% Triton X-100 for 10 min and incubated in CAS block solution (Life technologies) for 1 h at room temperature. TUNEL assay was performed using a TUNEL ApopTag® Peroxidase In Situ Apoptosis Detection Kit (Merck Millipore, Temecula, CA, S7100), according to the manufacturer's instructions.

Animals

Male BALB/c nude mice aged 4 weeks were purchased from Orient Bio Animal Inc. (Gyeonggido, Korea). All animal experiments were performed according to the guidelines of the INHA Institutional Animal Care and Use Committee (INHA IACUC) at the Medical School of Inha University, under the authority of project number INHA 200820-709-2. Animals were provided with standard chow and tap water *ad libitum*, and maintained under a 12 h dark/light cycle at 21°C under specific pathogen-free conditions. For tumor xenograft studies, male BALB/c nude mice (5 weeks old, weighing 18-20 g) were injected in the flank with 5×10^6 MIA PaCa-2 cells. When the tumor size reached approximately 50 mm^3, mice were randomly regrouped to ensure equal average tumor size among groups with different treatment conditions. One group of mice was left untreated, the second group received gemcitabine, the third group received KI-301690, and the fourth group received both gemcitabine and KI-301690. Treatment groups received gemcitabine (3 mg/kg) thrice a week and/or KI-301690 (30 mg/kg) five times a week, through intraperitoneal injection. Tumor size and body weight were measured 3 days per week, and tumor volume was calculated using Vernier calipers and the formula; 0.5 × length × $(width)^2$. After 45 days, tumors and other organs or tissues were carefully dissected to avoid contamination from surrounding tissues. For histological analysis, tissues were fixed in 10% paraformaldehyde, embedded in paraffin, and sectioned (in 3-μm sections).

Immunohistochemistry

Immunostaining was performed using 3-μm-thick sections of tumor samples after deparaffinization. Microwave antigen retrieval was performed in citrate buffer (pH 6.0) for 30 min and permeabilized with 0.5% Triton X-100 in PBS for 10 min. Peroxidase quenching was performed using 0.3% hydrogen peroxide (H_2O_2) in PBS for 10 min and preblocked with CAS block solution (Life technologies) for 1 h at room temperature. They were then incubated overnight with primary antibodies: anti-phospho DDR1, anti-phospho FAK, anti-Vimentin, anti-Collagen IV (Abcam, 6586), and anti-Ki67 (Abcam, 16667) at 4°C. For DAB staining, the sections were incubated for 1 h with biotinylated secondary antibodies (1:60) and streptavidin-HRP was applied. The sections were developed with diaminobenzidine tetrahydrochloride substrate, and counterstained with hematoxylin. For immunofluorescence, the sections were incubated for 1 h with fluorescently labeled secondary antibodies (1:60) and counterstained with 4,6-diamidino-2-phenylindole (DAPI) to visualize nuclei. At least three random fields in each section were examined × 200 magnification.

Ex vivo organotypic spheroids culture

5×10^6 MIA PaCa-2 cells were injected into the left flank of male BALB/c nude mice. The tumors were surgically removed at approximately 300-500 mm^3 in size, cut into 1 mm diameter sections, and explanted on 0.75% agarose-coated 24-well plates with a culture medium at 37°C. After overnight incubation, tumors were repetitively treated with KI-301690 for 2 days, KI-301690 and gemcitabine cotreatment for 3 days, and untreated for 2 days. After 14 days, the explants were harvested, fixed (10% PFA), and embedded in paraffin for histological analysis.

Statistical analysis

Statistical calculations were performed using SPSS software for Windows (version 10.0, SPSS, Chicago, IL, USA). Results are expressed as the mean ± standard deviation (SD) and are considered statistically significant at $*P < 0.05$, $**P < 0.01$, and $***P < 0.001$.

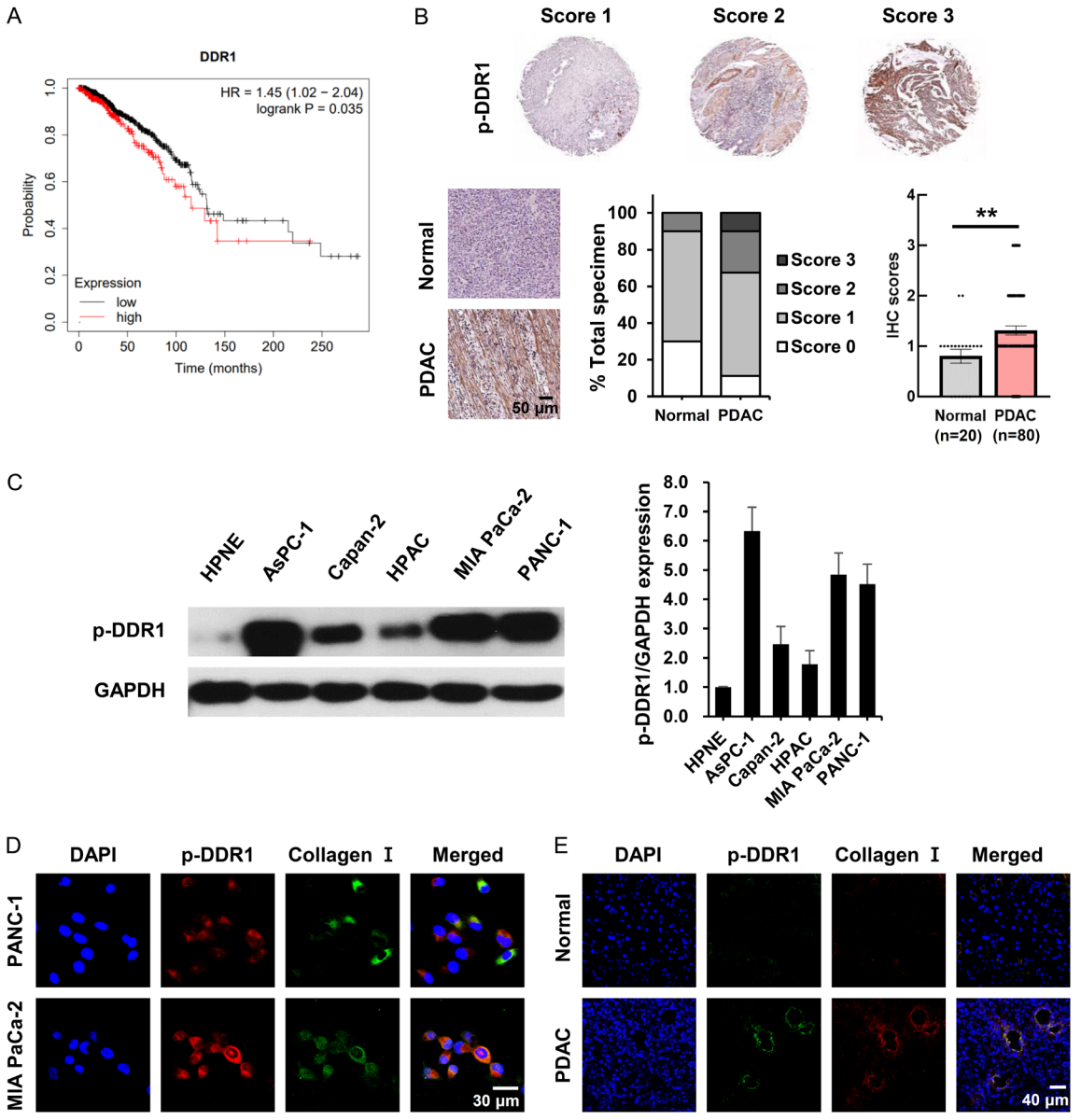

Figure 1. DDR1 expression in human pancreatic cancer. A. Kaplan-Meier analysis showed that high p-DDR1 expression was associated with poor overall survival in patients with pancreatic cancer. B. Representative immunohistochemical staining imaging of p-DDR1 in human PDAC tissue samples (n = 80). Scores were calculated based on intensity and percentage of stained cells. C. The expression of p-DDR1 in human normal pancreatic cell line (HPNE) and pancreatic cancer cell lines (AsPC-1, Capan-2, HPAC, MIA PaCa-2, and PANC-1). D and E. Expression of p-DDR1 and collagen I levels were analyzed using immunofluorescence staining in pancreatic cancer cells and MIA PaCa-2 orthotopic tumors. Data are presented as means ± standard deviation (**$P < 0.01$).

Results

Expression of p-DDR1 in pancreatic cancer patients

Kaplan-Meier analysis was used to determine the effect of DDR1 expression on the survival rate of patients with PDAC, as it affects tumor growth and progression [14, 15]. As shown in **Figure 1A**, patients with PDAC demonstrated a positive correlation between overall survival and DDR1 expression. Additionally, p-DDR1 expression was observed to be higher in patients with PDAC (**Figure 1B**). From western blotting analysis, we observed a significant increase in the expression of p-DDR1 in pancreatic cancer cells than in HPNE normal pancreatic cells (**Figure 1C**). Notably, co-expression

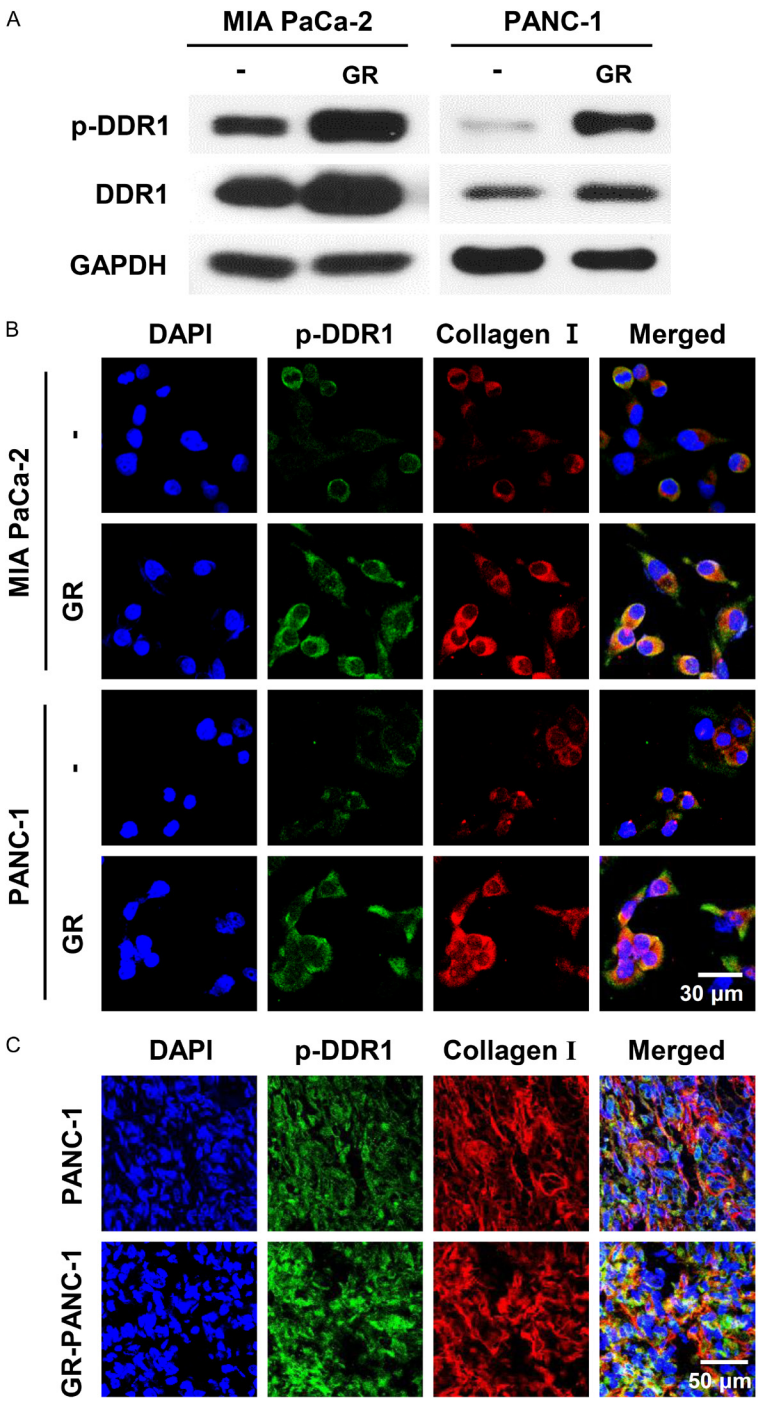

Figure 2. The high DDR1 expression in gemcitabine-resistant (GR) pancreatic cancer. A and B. Expressions of p-DDR1 and collagen in gemcitabine-resistant (GR) and naive cells using western blotting. These expressions were confirmed by immunofluorescence staining. C. High expressions of p-DDR1 and collagen I were observed in PANC-1 and PANC-1 GR tumors.

of p-DDR1 and collagen I was observed in pancreatic cancer cells (**Figure 1D**). These results were also confirmed in PDA tumor tissues (**Figure 1E**).

Expression of p-DDR1 in gemcitabine-resistant (GR) cells

DDR1 is a reported predictive factor for chemoresistance and a potential positive target for resistant cells [23]. Therefore, we investigated the association between DDR1 and acquired resistance to gemcitabine in pancreatic cancer cells and tumor tissues. As shown in **Figure 2A** and **2B**, DDR1 expression was highly upregulated in both MIA PaCa-2 gemcitabine-resistant (GR) cells and PANC-1/GR cells, compared to parental MIA PaCa-2 and PANC-1 cells. Additionally, we confirmed the elevated expressions of p-DDR1 and collagen I in GR-pancreatic cancer cells and PANC-1/GR tumors obtained from pancreatic mouse xenografts (**Figure 2B** and **2C**). These results demonstrate DDR1 involvement in gemcitabine resistance; therefore, DDR1 inhibition can increase gemcitabine sensitivity and overcome chemoresistance in pancreatic cancer.

Synthesis of a novel DDR1 inhibitor and its efficacy

We designed and synthesized KI-301690, a novel DDR1 inhibitor, and its binding mode was further investigated using Discovery Studio 4.5 software to gain an insight into its inhibitory effect (**Figure 3A** and **3B**). To obtain molecular insight into the inhibitory effect on KI-301690 toward DDR1, the binding mode was further investigated using the Discovery Studio 4.5 software. For the binding model, the DDR1 crystal structure (PDB code: 4CKR) was used as the molecular docking template, as shown in **Figure 3B**. In the most plausible model, the oxo-

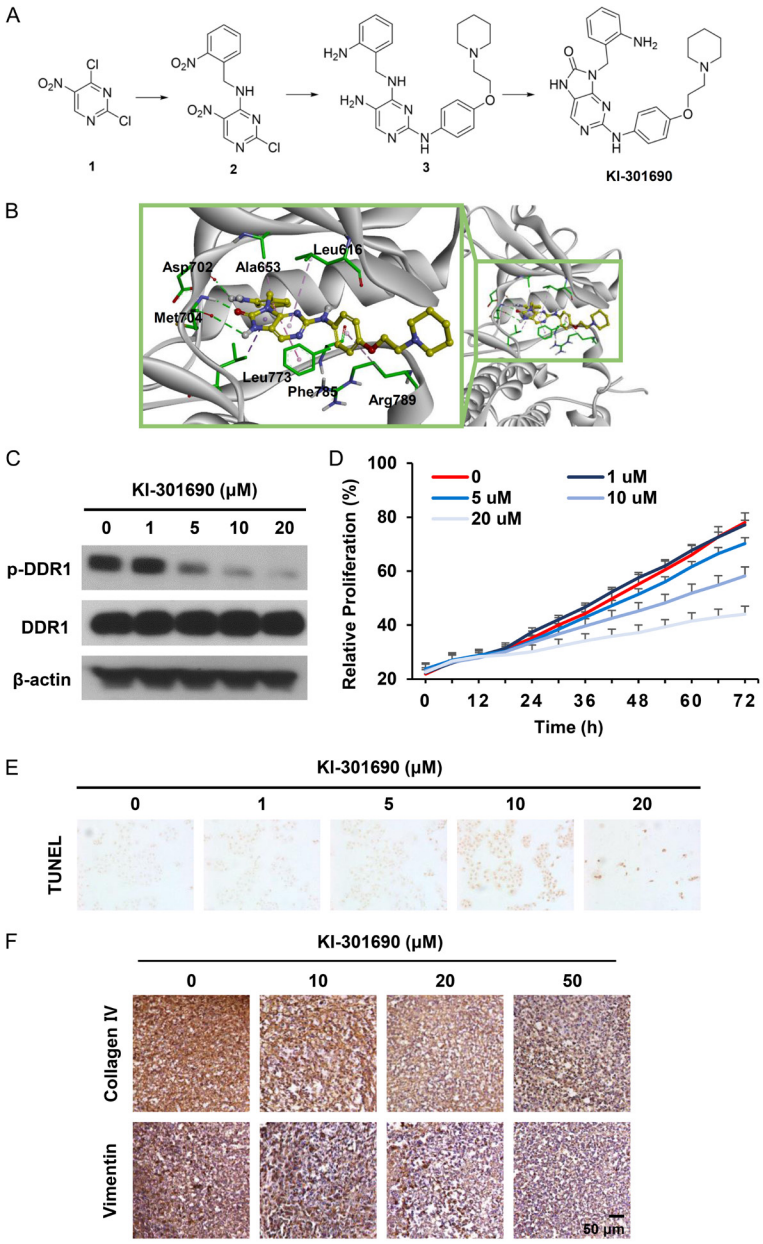

Figure 3. Characterization of KI-301690 and cytotoxic effect in pancreatic cancer cells. A and B. The chemical structure of KI-301690 and its binding mode. C. After PANC-1 cells were treated with KI-301690 (1-20 μM) for 24 h, the expression levels of p-DDR1 was determined using western blot analysis. D. KI-301690 effect on pancreatic cancer cell proliferation was estimated using a JULI™ stage real-time cell recorder. E. Induction of apoptosis by KI-301690 was assessed using TUNEL assay. F. Organotypic tumor spheroids cultured from xenograft tumor tissues (~2 mm in diameter) were treated with 10 μM KI-301690. Immunohistochemistry for collagen IV and vimentin. Data are presented as means ± standard deviation.

purine core forms two hydrogen bonds with Met704 in the hinge region and hydrophobics interaction with Leu616 and Leu773. Notably, aniline moiety forms an additional hydrogen bond with Asp702 in the hinge region and establishes hydrophobic interactions with Ala653 and Phe785. The synergistic hydrogen bonding and hydrophobic interactions generate a high affinity for DDR1. The piperidine group was directed toward the solvent region, and the phenyl group had close contact with the aliphatic chain of Arg789, which provides further binding stabilization.

KI-301690 was subjected to kinase selectivity profiling through a panel of 50 oncogenic kinases at 1 μM at Eurofins Pharma Discovery Services UK [www.eurofilns.com]. Of the tested kinases (**Table 1**), KI-301690 displayed the strongest binding affinity for DDR1 (percent of control [POC] = 9). Indeed, we found that KI-301690 inhibited p-DDR1 expression in a dose dependent manner in pancreatic cancer cells (**Figure 3C**). As KI-301690 induced specific DDR1 inhibition, its anti-proliferative effect in pancreatic cancer cells was assessed. When cells were exposed to various KI-301690 concentrations (1-20 μM) at different time points, we found decreased proliferative ability in PANC-1 cells in a dose and time-dependent manner (**Figure 3D**). Additionally, the apoptotic effect of KI-301690 was identified and its nuclear morphology was characterized using TUNEL assay and staining, respectively (**Figure 3E**). KI-301690 regulated ECM production by inhibiting the expressions of major ECM components such as collagen IV and vimentin (**Figure 3F**). Given that DDR1 was highly expressed in pancreatic cancer with an abundance of ECM and pancreatic tumors with GR and that KI-301690 effectively inhibited expressions of major ECM com-

Table 1. Representative kinase profile of KI-301690

Kinase name	Percent of Control (POC)	Compound dose (nM)	Kinase name	Percent of Control (POC)	Compound dose (nM)
DDR1	9	1000	JAK1	100	1000
DDR2	103	1000	JAK2	73	1000
ALK	95	1000	LKB1	112	1000
AMPKα1	103	1000	MAPK1	112	1000
Aurora-A	109	1000	MEK1	96	1000
Aurora-B	99	1000	Met	104	1000
Aurora-C	101	1000	p70S6K	103	1000
Axl	108	1000	PAK1	101	1000
Blk	59	1000	PDGFRα	89	1000
Bmx	79	1000	PDGFRβ	91	1000
B-Raf	102	1000	Pim-1	101	1000
c-RAF	97	1000	PKBα	106	1000
DAPK1	100	1000	PKCα	99	1000
DYRK2	103	1000	Plk1	147	1000
EGFR	97	1000	Ret	97	1000
ErbB2	106	1000	ROCK-I	109	1000
FAK	95	1000	TAK1	106	1000
Fer	117	1000	Tie2	94	1000
Fes	63	1000	Wee1	101	1000
FGFR1	97	1000	DNA-PK	105	1000
FGFR2	104	1000	PI3 Kinase (p110b/p85a)	96	1000
Flt1	97	1000	PI3 Kinase (p120g)	97	1000
GSK3β	104	1000	PI3 Kinase (p110d/p85a)	96	1000
IGF-1R	101	1000	PI3 Kinase (p110a/p85a)	97	1000
IKKβ	112	1000	Fms	30	1000

KI-301690 was subjected to kinase selectivity profiling with a panel of 50 oncogenic kinases at 1 μM at the Eurofins Pharma Discovery Services UK [www.eurofins.com]. Of the kinases tested, KI-301690 displayed strongest binding affinity to DDR1 (POC = 9).

ponents by binding collagen, we expected that KI-301690 could increase gemcitabine sensitivity when used in combination.

Induction of apoptosis in pancreatic cancer cells by combination treatment of KI-301690 and gemcitabine

To determine whether KI-301690 enhanced the cancer cell-killing effect of gemcitabine, we analyzed the viability of pancreatic cancer cells using MTT assay, following combined KI-301690 and gemcitabine treatment. Cells were treated with gemcitabine (0.1 and 0.5 μM) alone or with KI-301690 (10 and 20 μM) for 72 h. Compared to treatment with either agent alone, the combination of KI-301690 and gemcitabine synergistically inhibited growth in the two human pancreatic cancer cell lines (**Figure 4A**). To validate the synergistic effect of KI-301690 and gemcitabine, we further examined the combination index (CI) values using CalcuSyn software. The combination of 10 μM KI-301690 and 0.5 μM gemcitabine produced significant synergistic effects, (CI values < 1) in PANC-1 (CI = 0.50) and MIA PaCa-2 (CI = 0.87) cells (**Figure 4B**). Because the combined treatment significantly reduced cell viability, we next investigated the apoptotic effect of combination treatment. First, we performed cytochrome c and JC-1 staining to identify the involvement of the combined treatment in MMP changes, which induced mitochondrial cytochrome c release. The combined treatment synergistically increased cytochrome c release with a concomitant decrease in cytochrome c and mitochondria colocalization (**Figure 4C**). With JC-1 staining, combined treatment induced marked changes in MMP, as evidenced by a clear decrease in red fluorescence or increase

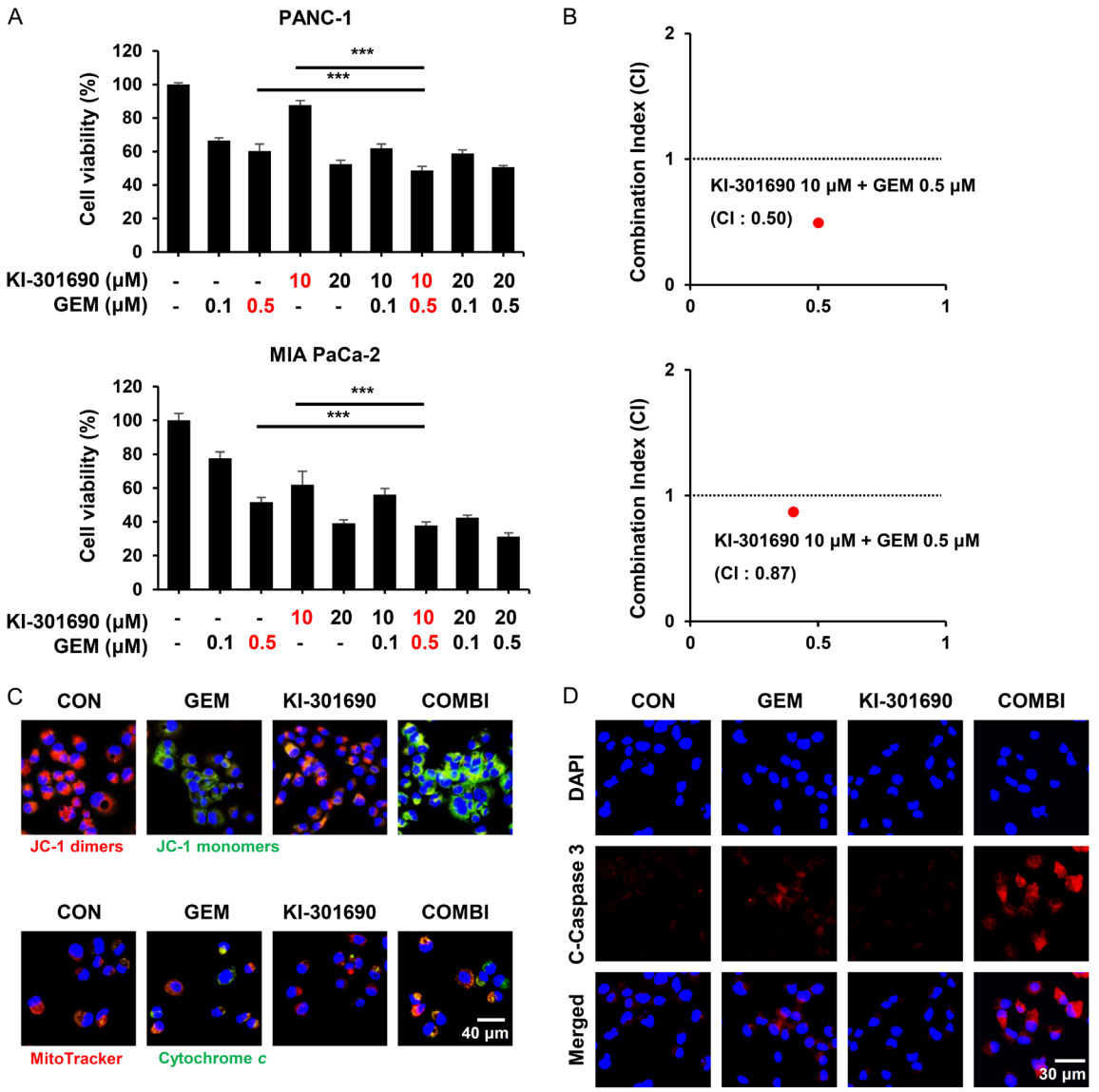

Figure 4. Synergistic cytotoxic effect of KI-301690 and gemcitabine in pancreatic cancer cells. A. PANC-1 and MIA PaCa-2 cells were treated with KI-301690 and/or gemcitabine for 72 h. MTT assay was performed to determine the cytotoxic effects of KI-301690 and gemcitabine. B. The combination of gemcitabine (0.5 μM) and KI-301690 (10 μM) showed a synergistic effect. CI values for KI-301690 and gemcitabine were determined using CompuSyn software. A CI value < 1 was indicative of a synergistic effect. The combination treatment showed a synergistic effect in both cell lines, as reflected in the corresponding CI values of 0.5 and 0.87, respectively. C. Fluorescence images of JC-1 aggregates (red) and monomers in PANC-1 cells after treatment with KI-301690 and gemcitabine for 12 h. Results were analyzed by plotting the ratio of depolarized cells to polarized cells. After treatment with KI-301690 and/or gemcitabine for 12 h, PANC-1 cells were stained with anti-cytochrome *c* antibodies, MitoTracker and DAPI, and analyzed under an Olympus confocal laser-scanning microscope. D. Induction of apoptosis by the combination treatment was determined in PANC-1 cells by performing cleaved caspase-3 (red) staining. Data are presented as the mean ± standard deviation (***$P < 0.001$).

in green fluorescence. Additionally, it increased the expression of cleaved caspase-3, a prominent apoptotic protein (**Figure 4D**). Our results suggest that the synergistic effects of KI-301690 combined with gemcitabine were induced by mitochondrial-mediated apoptosis in PDAC cells.

Combination treatment of KI-301690 and gemcitabine inhibits cell migration and invasion

As cancer cell migration and invasion are prerequisites for metastasis, we performed migration and invasion assays in PANC-1 cells to

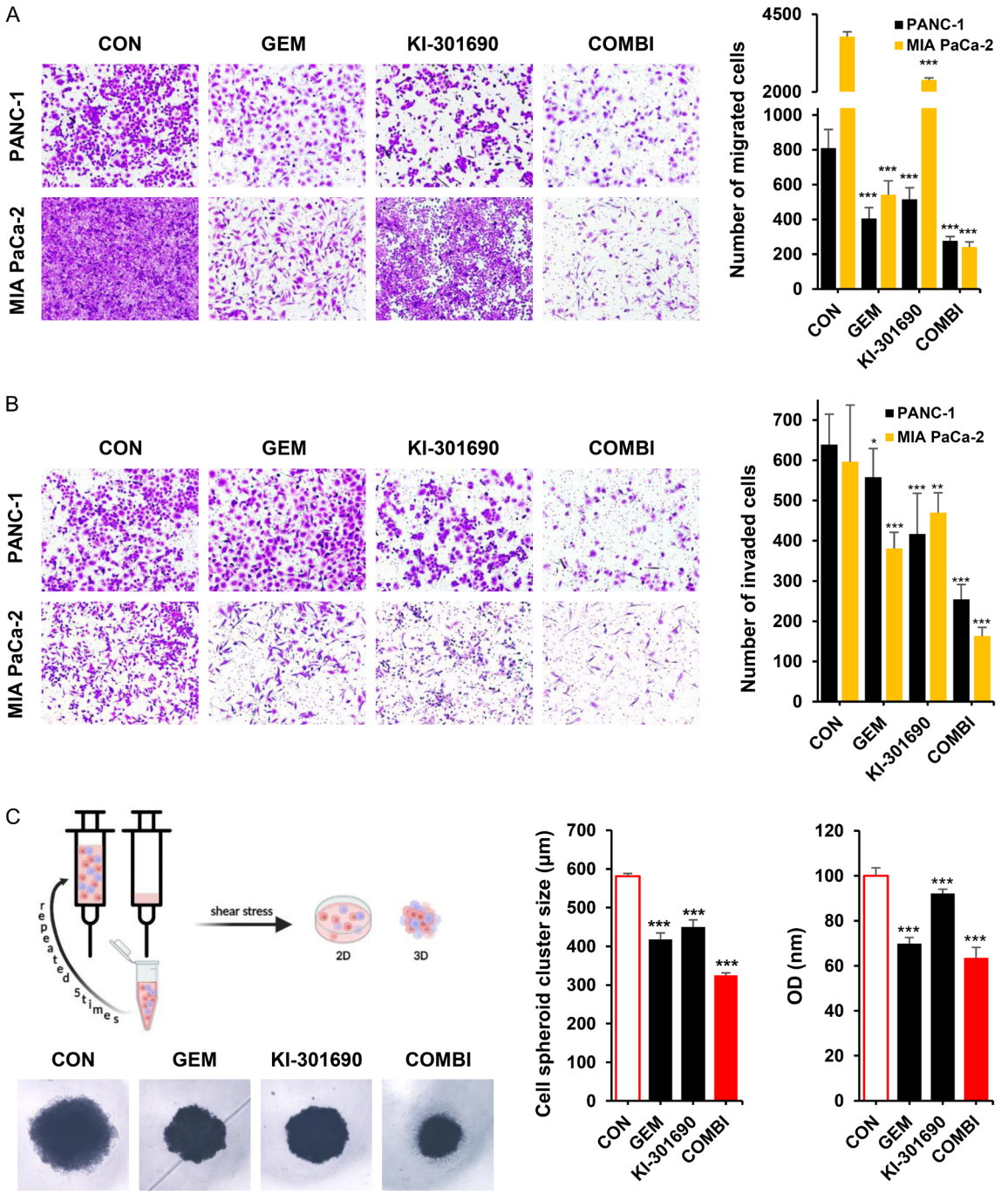

Figure 5. Inhibition of metastatic pancreatic cancer by the combined treatment of KI-301690 and gemcitabine. A and B. Ability of metastatic pancreatic cancer cells was assessed using a Transwell migration and invasion assay. Cells were seeded in the upper chamber after KI-301690 treatment and the lower chamber was treated with gemcitabine for 72 h. The number of migrated or invaded cells were counted using counted using ImageJ software. C. Schematic representation of fluid shear stress assay, another metastatic *in vitro* model. Three-dimensional spheroid cluster assay was carried out 11 days after exposure to shear stress of PANC-1 cells with the combination treatment. Data are presented as means ± standard deviation (**P* < 0.05, ***P* < 0.01, and ****P* < 0.001 *vs* CON).

determine KI-301690 and gemcitabine co-treatment inhibition. The migration of PANC1 and MIA PaCa-2 cells was synergistically inhibited in Boyden Chamber assays (**Figure 5A**). Similarly, this combination significantly inhibited the invasion of both cell lines more than that of the control and treated groups (**Figure 5B**). Subsequently, we investigated

whether the combined treatment inhibited the viability of cells in response to shear stress and anchorage-independent growth (cell cluster), which circulating tumor cells undergo *in vivo*. As shown in **Figure 5C**, we found that cell spheroid growth on collagen-coated plates was significantly decreased with combined treatment, than in single treatment, suggesting that the combination of KI-301690 and gemcitabine inhibited pancreatic cancer metastasis.

Inhibition of ECM components by combination treatment with KI-301690 and gemcitabine via blockade of DDR1/PYK2/FAK signaling in pancreatic cancer cells

Pancreatic cancer is characterized by collagen-rich and fibrillary collagens (collagen I and collagen IV), which accelerate tumor progression. As DDR1 is known to activate ECM formation and signaling, we assessed whether combined treatment with KI-301690 and gemcitabine was effectively capable of modulating major ECM components such as collagen IV, fibronectin, vimentin, and α-SMA in *ex vivo* tumors. KI-301690 reduced the expression of ECM components compared with the control or gemcitabine alone, but the combination treatment potently decreased the expression of various ECM components, including collagen IV (**Figure 6A** and **6B**). To identify the mechanism responsible for ECM inhibition by the combined treatment together with anti-proliferative and apoptotic effects in pancreatic cancer cells, we investigated the effect on DDR1 signaling pathways, including proline-rich tyrosine kinase 2 (PYK2) and FAK. The immunofluorescence results confirmed that the combined treatment inhibited expressions of p-DDR1, p-PYK2, p-FAK, collagen I (**Figure 6C** and **6D**). Furthermore, based on previous studies reporting that ECM components function as a physical barrier that prevents drug diffusion, leading to abysmal therapeutic outcomes [24], we investigated whether KI-301690 improved anti-cancer drug delivery such as doxorubicin (DOX, red color) through ECM reduction. The combined treatment effectively increased the delivery and distribution of the drug through the formation of mature blood vessels (VWF, green) by reducing the production of ECM components (**Figure 6E**), by the inhibition of collagen-mediated DDR1 signaling including PYK2 and FAK; resulting in the improved drug delivery and diffusion in pancreatic cancer cells.

Antitumor effects of combination treatment with KI-301690 and gemcitabine in a pancreatic cancer xenograft model

To assess whether KI-301690 enhanced the efficacy of chemotherapy in a PDAC xenograft model, mice were injected intraperitoneally with 30 mg/kg KI-301690 and gemcitabine (3 mg/kg) for 45 days. The tumor growth of mice treated with KI-301690 or gemcitabine alone was delayed compared with that of the control group. However, the combination of KI-301690 and gemcitabine significantly reduced the tumor volume by 64% as compared to that in the control group, which was consistent with the changes in tumor weight (**Figure 7A**). Histopathologically, the combination treatment showed a decrease in KI-67, a cell proliferation marker, and induced apoptosis by increasing the expression of cleaved caspase-3 (**Figure 7B**). Additionally, combination treatment significantly attenuated intratumoral expression of major ECM components such as collagen IV and fibronectin (**Figure 7C**), which are associated with the inhibition of drug diffusion in tumor beds. Moreover, it effectively decreased the expression of p-DDR, p-PYK2, and p-FAK.

Discussion

PDAC is characterized by a desmoplastic response that results in dense deposition of the ECM, which is known to promote cancer progression. Emerging evidence has shown that the ECM is important for establishing resistant niches by allowing cancer cells to rapidly tolerate therapeutic drugs before mutagenic resistance mechanisms are acquired [25, 26]. Collagen, the most abundant fibrous protein component in the ECM, directly binds to DDR1, and DDR1-collagen signaling is known to be involved in cancer cell migration, invasion, and tumorigenesis. Additionally, it has been closely linked to low sensitivity to chemotherapy and drug resistance [19, 21]. We observed a high expression of DDR1 in GR-PDAC cells, suggesting the role of DDR1 in implementing rapid adaptive responses to cytotoxic agents such as gemcitabine. Therefore, based on previous studies demonstrating that genetic and pharmacological inhibition of DDR1 induced effec-

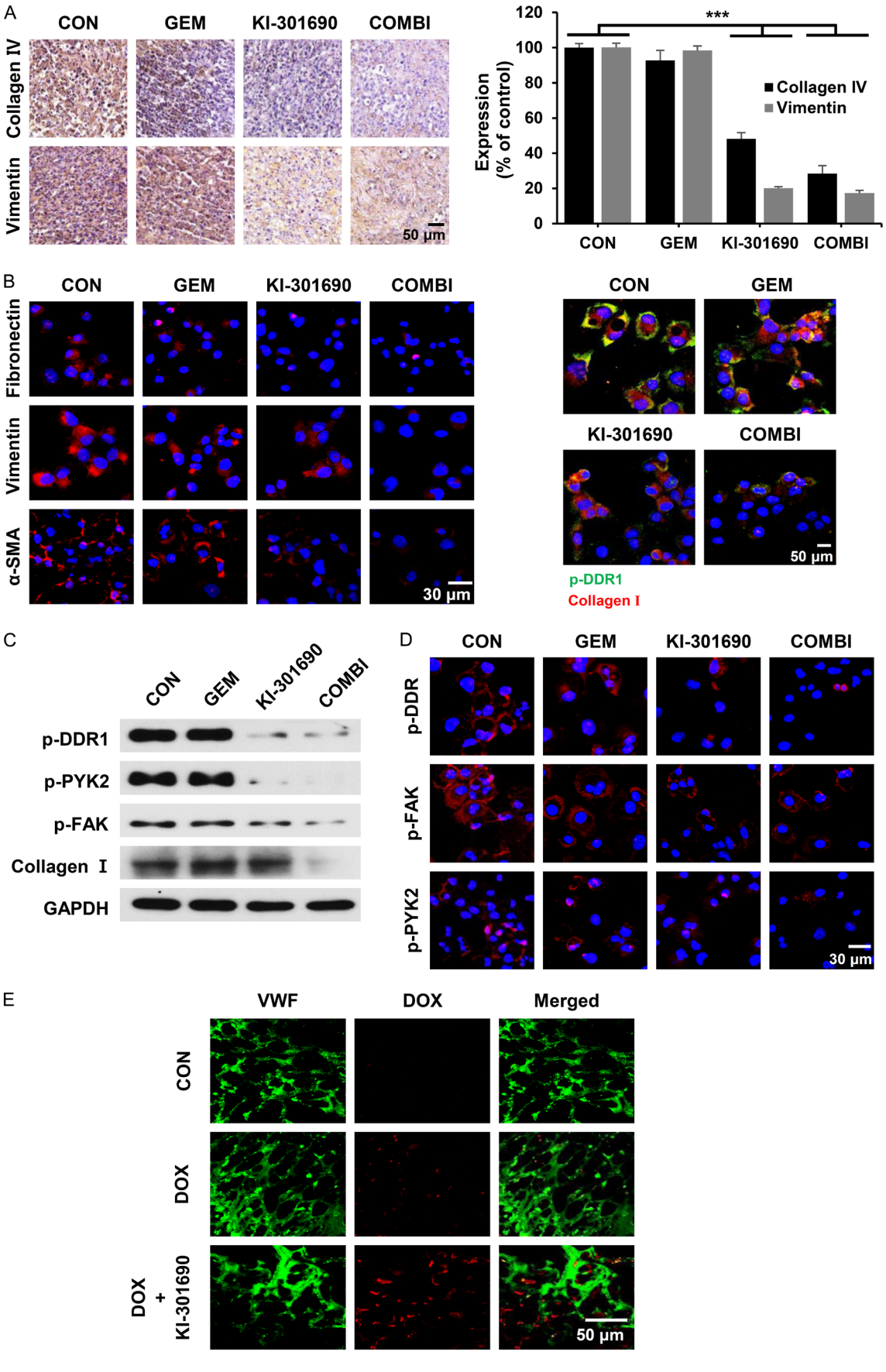
A
CON
GEM
KI-301690
COMBI
Collagen IV
Vimentin
50 μm
***
Expression (% of control)
120
100
80
60
40
20
0
Collagen IV
Vimentin
CON
GEM
KI-301690
COMBI
B
CON
GEM
KI-301690
COMBI
Fibronectin
Vimentin
α-SMA
30 μm
CON
GEM
KI-301690
COMBI
50 μm
p-DDR1
Collagen I
C
CON
GEM
KI-301690
COMBI
p-DDR1
p-PYK2
p-FAK
Collagen I
GAPDH
D
CON
GEM
KI-301690
COMBI
p-DDR
p-FAK
p-PYK2
30 μm
E
VWF
DOX
Merged
CON
DOX
DOX + KI-301690
50 μm

Figure 6. Inhibition of the ECM accumulation through blocking of DDR1/PYK/FAK signaling by the combined treatment. A. Expressions of ECM components including collagen IV and vimentin in organotrophic tumor spheroids cultured from xenograft tumor tissues. B. PANC-1 cells were treated with gemcitabine (0.5 μM) and/or KI-301690 (10 μM) for 48 h and the expressions of ECM components and p-DDR1 were evaluated. C and D. After PANC-1 cells were treated with gemcitabine (0.5 μM) and/or KI-301690 (10 μM) for 48 h, the expression levels of p-DDR1, p-PYK2, p-FAK and collagen I were determined using western blot analysis and immunofluorescence staining. E. After combination treatment of KI-301690 with doxorubicin (DOX) in PANC-1 cells xenograft models, delivery and distribution of DOX was increased by the efficacy of KI-301690 to reduce ECM (***$P < 0.001$).

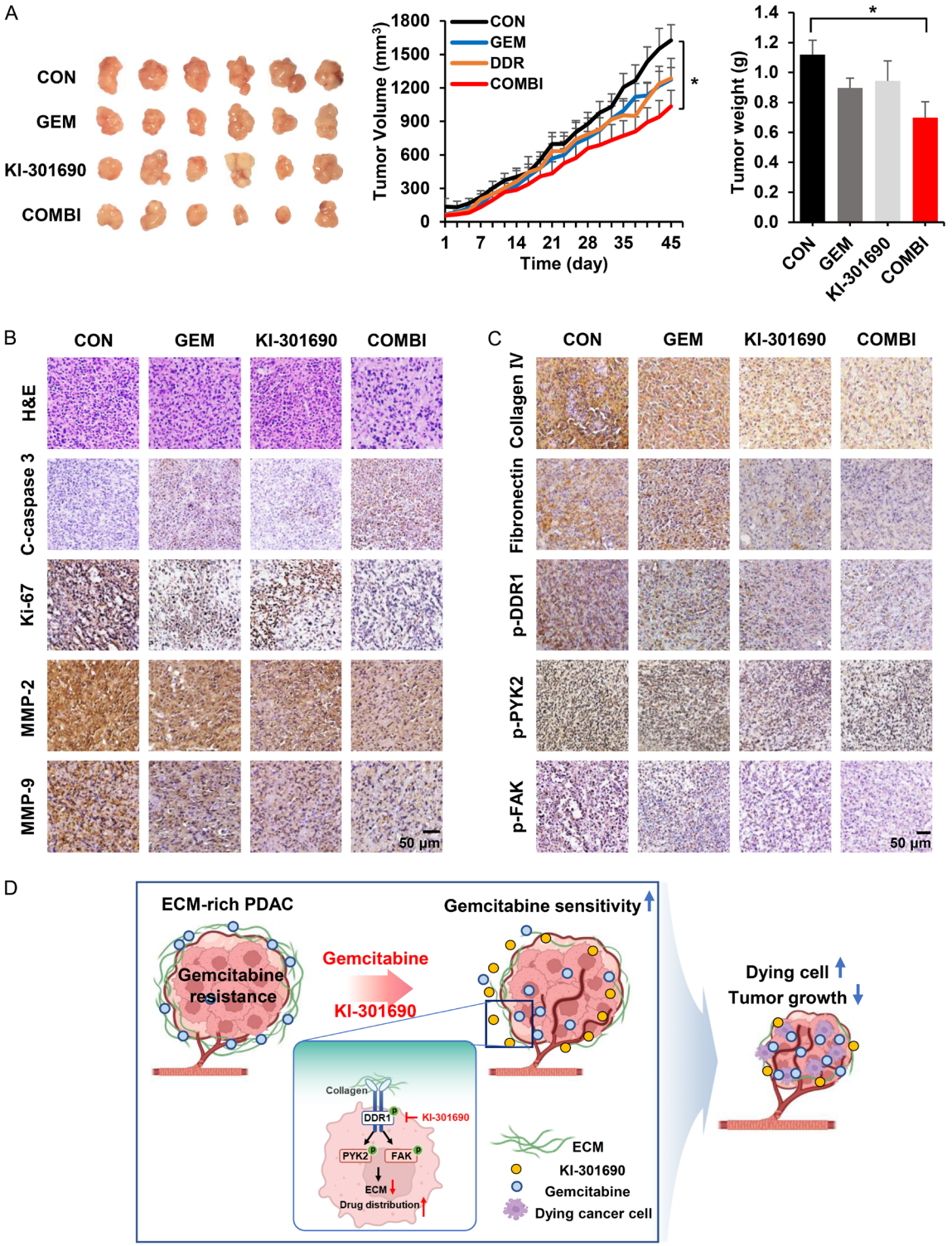

Figure 7. Effect of the combination treatment in pancreatic cancer xenograft models. A. The antitumor efficacy of the combination treatment of KI-301690 and gemcitabine was analyzed by measuring the tumor volume and weights in MIA PaCa-2 pancreatic cancer xenograft models. Mice were administered 30 mg/kg KI-301690 five times a week and 3 mg/kg gemcitabine thrice weekly by intraperitoneal injections, for 45 days (n = 6). B and C. Histological analysis of pancreatic xenograft tumor tissue using hematoxylin and eosin (H&E) staining, immunohistochemical detection of cleaved caspase-3, KI-67, MMP-2, MMP-9, ECM components (collagen IV and fibronectin), and molecules of DDR1 signaling (p-DDR1, p-PYK2, and p-FAK). D. Scheme for how KI-301690 combined with gemcitabine inhibits ECM production and the growth of pancreatic cancer. Data are presented as the mean ± standard deviation (*$P < 0.05$).

tive therapeutic results in drug sensitivity and resistance [23, 27-30], we synthesized and characterized KI-301690, a novel DDR1 inhibitor, and evaluated its anti-cancer efficacy in combination with gemcitabine in PDAC cells. Our results revealed that KI-301690 inhibited ECM accumulation by DDR1 signaling pathway blockade, which further synergistically enhanced gemcitabine efficacy in PDAC.

KI-301690 is a small molecule that disrupts DDR1 signaling by targeting its ATP-binding site, and its kinase profile analysis revealed that it was a selective DDR1 inhibitor with 91% inhibition, suggesting that it was DDR1-specific with minimal off-target effects. Although several DDR1 inhibitors have been developed, they have not been approved for clinical application due to a broad inhibition of several kinases with limited potency [31]. Furthermore, few studies have verified their efficacy in combination therapy with other chemo-agents. As DDR1 is associated with chemoresistance [27-29] and a high expression of DDR1 was observed in GR cells and tumors in this study, we expected that KI-301690 could increase gemcitabine sensitivity in PDAC combination treatment and improve the acquired resistance of gemcitabine. Our results showed that the combination of KI-301690 and gemcitabine significantly inhibited the growth of pancreatic cancer cells compared to treatment with either agent alone. It elicited a significant increase in apoptosis through the increased cleaving of caspase-3 in pancreatic cancer than in either treatment alone. The combination treatment induced marked changes in MMP and synergistically increased cytochrome *c* release, which was consistent with the results of Nokin *et al*. that DDR1 inhibitor increased apoptosis in combination with cisplatin in lung cancer [23]. These observations were supported by *in vivo* experiments showing that combination treatment increased cleaved caspase-3-positive cell populations, thereby delaying tumor growth in a pancreatic cancer xenograft model. In addition to its apoptotic effect, this combination inhibited the migration and invasion of pancreatic cancer cells. Previous studies showed that DDR1 overexpression increased migration and invasion of cancer cells and its depletion caused a decrease [32-34]. Therefore, this combination effect is believed to be due to enhancement of the anti-migration/invasive efficacy of gemcitabine by KI-301690.

DDR1 is an RTK activated by the ECM protein collagen and is known as an important factor in ECM production [35]. It promotes tumor progression and metastasis; however, the exact mechanism is still unclear. Shintani *et al.* have reported that DDR1 directly interacts with PYK2. Upon collagen-mediated DDR1 kinase activation, PYK2 phosphorylation occurs to regulate cancer cell proliferation and metastasis related genes [36]. FAK, one of the downstream signals of DDR1, is an important intracellular molecule in signal transduction from the ECM to the cell, and the level of constitutive FAK phosphorylation correlates with gemcitabine resistance in PDAC [37]. Therefore, we identified that the combination of KI-301690 with gemcitabine affected DDR1-mediated PYK2/FAK signaling and decreased the ECM. In this study, efficient inhibition of collagen I/IV and other major ECM components was observed in pancreatic cancer cell and tumor tissues treated with KI-301690 and gemcitabine.

This combination effectively increased p-PYK2 and p-FAK inhibition by targeting DDR1 by KI-301690. Interestingly, reduced collagen deposition in tumors of mice treated with KI-301690 and improved drug delivery were confirmed by observing doxorubicin. Given that desmoplastic matrix interferes with drug delivery, as a determinant of chemotherapy resistance and a potential target for PDAC therapy, this result proves that the DDR1-collagen interaction contributes to drug resistance and can be improved through DDR1 inhibition. Although

the combination of KI-301690 and gemcitabine inhibited the expression of ECM components and improved drug delivery through DDR1/PYK2/FAK signaling inhibition, further studies are required to determine mechanism of DDR1 signaling regulation in the inhibition of ECM production and drug resistance.

In conclusion, our results demonstrate that KI-301690-mediated loss of ECM by DDR1 signal inhibition can restore chemosensitivity toward gemcitabine, resulting in pancreatic tumor growth inhibition. Therefore, we recommend the combination of KI-301690 and gemcitabine as a promising strategy for overcoming tumor-induced drug resistance and inducing potent antitumor effects in highly ECM-rich pancreatic cancer (**Figure 7D**).

Acknowledgements

This research was supported by the National Research Foundation of Korea (2021R1A2B5B03086410, 2021R1A5A2031612, 2019M3E5D1A02069621), the Institute for Basic Science (IBS-R010-A2), and Korea Institute of Science and Technology (2E30240).

Disclosure of conflict of interest

None.

Address correspondence to: Dr. Soon-Sun Hong, Department of Medicine, College of Medicine, and Program in Biomedical Science & Engineering, Inha University, 3-ga, Sinheung-dong, Jung-gu, Incheon 22332, Korea. Tel: +82-32-890-3683; E-mail: hongs@inha.ac.kr; Dr. Sungwoo Hong, Center for Catalytic Hydrocarbon Functionalization, Institute of Basic Science (IBS) and Department of Chemistry, Korea Advanced Institute of Science and Technology (KAIST), Daejeon 34141, Korea. Tel: +82-32-890-3683; E-mail: hongorg@kaist.ac.kr; Dr. So Ha Lee, Chemical Kinomics Research Center, Korea Institute of Science and Technology, Seoul 02792, Korea. Tel: +82-2-958-6834; E-mail: lsh6211@kist.re.kr

References

[1] Ryan DP, Hong TS and Bardeesy N. Pancreatic adenocarcinoma. N Engl J Med 2014; 371: 1039-1049.

[2] Bednar F and Simeone DM. Recent advances in pancreatic surgery. Curr Opin Gastroenterol 2014; 30: 518-523.

[3] Ghaneh P, Smith R, Tudor-Smith C, Raraty M and Neoptolemos JP. Neoadjuvant and adjuvant strategies for pancreatic cancer. Eur J Surg Oncol 2008; 34: 297-305.

[4] Conroy T, Desseigne F, Ychou M, Bouché O, Guimbaud R, Bécouarn Y, Adenis A, Raoul JL, Gourgou-Bourgade S, de la Fouchardière C, Bennouna J, Bachet JB, Khemissa-Akouz F, Péré-Vergé D, Delbaldo C, Assenat E, Chauffert B, Michel P, Montoto-Grillot C and Ducreux M; Groupe Tumeurs Digestives of Unicancer; PRODIGE Intergroup. FOLFIRINOX versus gemcitabine for metastatic pancreatic cancer. N Engl J Med 2011; 364: 1817-1825.

[5] Romanus D, Kindler HL, Archer L, Basch E, Niedzwiecki D, Weeks J and Schrag D; Cancer and Leukemia Group B. Does health-related quality of life improve for advanced pancreatic cancer patients who respond to gemcitabine? Analysis of a randomized phase III trial of the cancer and leukemia group B (CALGB 80303). J Pain Symptom Manage 2012; 43: 205-217.

[6] Sultana A, Smith CT, Cunningham D, Starling N, Neoptolemos JP and Ghaneh P. Meta-analyses of chemotherapy for locally advanced and metastatic pancreatic cancer. J Clin Oncol 2007; 25: 2607-2615.

[7] Shields MA, Dangi-Garimella A, Redig AJ and Munshi HG. Biochemical role of the collagen-rich tumour microenvironment in pancreatic cancer progression. Biochem J 2012; 441: 541-52.

[8] Cox TR. The matrix in cancer. Nat Rev Cancer 2021; 21: 217-238.

[9] Poltavets V, Kochetkova M, Pitson SM and Samuel MS. The role of the extracellular matrix and its molecular and cellular regulators in cancer cell plasticity. Front Oncol 2018; 8: 431.

[10] Alves F, Vogel W, Mossie K, Millauer B, Höfler H and Ullrich A. Distinct structural characteristics of discoidin I subfamily receptor tyrosine kinases and complementary expression in human cancer. Oncogene 1995; 10: 609-618.

[11] Henriet E, Sala M, Hammoud AA, Tuariihionoa A, Martino JD, Ros M and Saltel F. Multitasking discoidin domain receptors are involved in several and specific hallmarks of cancer. Cell Adh Migr 2018; 12: 363-377.

[12] Gao H, Chakraborty G, Zhang Z, Akalay I, Gadiya M, Gao Y, Sinha S, Hu J, Jiang C, Akram M, Brogi E, Leitinger B and Giancotti FG. Multi-organ site metastatic reactivation mediated by non-canonical discoidin domain receptor 1 signaling. Cell 2016; 166: 47-62.

[13] Jin H, Ham IH, Oh HJ, Bae CA, Lee D, Kim YB, Son SY, Chwae YJ, Han SU, Brekken RA and Hur H. Inhibition of discoidin domain receptor

1 prevents stroma-induced peritoneal metastasis in gastric carcinoma. Mol Cancer Res 2018; 16: 1590-1600.
[14] Quan J, Yahata T, Adachi S, Yoshihara K and Tanaka K. Identification of receptor tyrosine kinase, discoidin domain receptor 1 (DDR1), as a potential biomarker for serous ovarian cancer. Int J Mol Sci 2011; 12: 971-982.
[15] Valencia K, Ormazábal C, Zandueta C, Luis-Ravelo D, Antón I, Pajares MJ, Agorreta J, Montuenga LM, Martínez-Canarias S, Leitinger B and Lecanda F. Inhibition of collagen receptor discoidin domain receptor-1 (DDR1) reduces cell survival, homing, and colonization in lung cancer bone metastasis. Clin Cancer Res 2012; 18: 969-980.
[16] Huo Y, Yang M, Liu W, Yang J, Fu X, Liu D, Li J, Zhang J, Hua R and Sun Y. High expression of DDR1 is associated with the poor prognosis in Chinese patients with pancreatic ductal adenocarcinoma. J Exp Clin Cancer Res 2015; 34: 88.
[17] Lee YC, Kurtova AV, Xiao J, Nikolos F, Hayashi K, Tramel Z, Jain A, Chen F, Chokshi M, Lee C, Bao G, Zhang X, Shen J, Mo Q, Jung SY, Rowley D and Chan KS. Collagen-rich airway smooth muscle cells are a metastatic niche for tumor colonization in the lung. Nat Commun 2019; 10: 2131.
[18] Ongusaha PP, Kim JI, Fang L, Wong TW, Yancopoulos GD, Aaronson SA and Lee SW. p53 induction and activation of DDR1 kinase counteract p53-mediated apoptosis and influence p53 regulation through a positive feedback loop. EMBO J 2003; 22: 1289-1301.
[19] Cader FZ, Vockerodt M, Bose S, Nagy E, Brundler MA, Kearns P and Murray PG. The EBV oncogene LMP1 protects lymphoma cells from cell death through the collagen-mediated activation of DDR1. Blood 2013; 122: 4237-4245.
[20] Lai SL, Tan ML, Hollows RJ, Robinson M, Ibrahim M, Margielewska S, Parkinson SK, Ramanathan A, Zain RB, Mehanna H, Spruce RJ, Wei W, Chung I, Murray PG, Yap LF and Paterson IC. Collagen induces a more proliferative, migratory and chemoresistant phenotype in head and neck cancer via DDR1. Cancers (Basel) 2019; 11: 1766.
[21] Deng Y, Zhao F, Hui L, Li X, Zhang D, Lin W, Chen Z and Ning Y. Suppressing miR-199a-3p by promoter methylation contributes to tumor aggressiveness and cisplatin resistance of ovarian cancer through promoting DDR1 expression. J Ovarian Res 2017; 10: 50.
[22] Ye L, Pu C, Tang J, Wang Y, Wang C, Qiu Z, Xiang T, Zhang Y and Peng W. Transmembrane-4 L-six family member-1 (TM4SF1) promotes non-small cell lung cancer proliferation, invasion and chemo-resistance through regulating the DDR1/Akt/ERK-mTOR axis. Respir Res 2019; 20: 106.
[23] Nokin MJ, Darbo E, Travert C, Drogat B, Lacouture A, José SS, Cabrera N, Turcq B, Prouzet-Mauleon V, Falcone M, Villanueva A, Wang H, Herfs M, Mosteiro M, Jänne PA, Pujol JL, Maraver A, Barbacid M, Nadal E, Santamaría D and Ambrogio C. Inhibition of DDR1 enhances in vivo chemosensitivity in KRAS-mutant lung adenocarcinoma. JCI Insight 2020; 5: e137869.
[24] Shields MA, Dangi-Garimella S, Krantz SB, Bentrem DJ and Munshi HG. Pancreatic cancer cells respond to type I collagen by inducing snail expression to promote membrane type 1 matrix metalloproteinase-dependent collagen invasion. J Biol Chem 2011; 286: 10495-10504.
[25] Meads MB, Gatenby RA and Dalton WS. Environment-mediated drug resistance: a major contributor to minimal residual disease. Nat Rev Cancer 2009; 9: 665-674.
[26] Smith MP, Brunton H, Rowling EJ, Ferguson J, Arozarena I, Miskolczi Z, Lee JL, Girotti MR, Marais R, Levesque MP, Dummer R, Frederick DT, Flaherty KT, Cooper ZA, Wargo JA and Wellbrock C. Inhibiting drivers of non-mutational drug tolerance is a salvage strategy for targeted melanoma therapy. Cancer Cell 2016; 29: 270-284.
[27] Ambrogio C, Gómez-López G, Falcone M, Vidal A, Nadal E, Crosetto N, Blasco RB, Fernández-Marcos PJ, Sánchez-Céspedes M, Ren X, Wang Z, Ding K, Hidalgo M, Serrano M, Villanueva A, Santamaría D and Barbacid M. Combined inhibition of DDR1 and Notch signaling is a therapeutic strategy for KRAS-driven lung adenocarcinoma. Nat Med 2016; 22: 270-277.
[28] Villalba M, Redin E, Exposito F, Pajares MJ, Sainz C, Hervas D, Guruceaga E, Diaz-Lagares A, Cirauqui C, Redrado M, Valencia K, de Andrea C, Jantus-Lewintre E, Camps C, Lopez-Lopez R, Lahoz A, Montuenga L, Pio R, Sandoval J and Calvo A. Identification of a novel synthetic lethal vulnerability in non-small cell lung cancer by co-targeting TMPRSS4 and DDR1. Sci Rep 2019; 9: 15400.
[29] Zhavoronkov A, Ivanenkov YA, Aliper A, Veselov MS, Aladinskiy VA, Aladinskaya AV, Terentiev VA, Polykovskiy DA, Kuznetsov MD, Asadulaev A, Volkov Y, Zholus A, Shayakhmetov RR, Zhebrak A, Minaeva LI, Zagribelnyy BA, Lee LH, Soll R, Madge D, Xing L, Guo T and Aspuru-Guzik A. Deep learning enables rapid identification of potent DDR1 kinase inhibitors. Nat Biotechnol 2019; 37: 1038-1040.
[30] Berestjuk I, Lecacheur M, Carminati A, Diazzi S, Rovera C, Prod'homme V, Ohanna M, Popovic A, Mallavialle A, Larbret F, Pisano S, Audebert S, Passeron T, Gaggioli C, Girard CA,

Deckert M and Tartare-Deckert S. Targeting discoidin domain receptors DDR1 and DDR2 overcomes matrix-mediated tumor cell adaptation and tolerance to BRAF-targeted therapy in melanoma. EMBO Mol Med 2022; 14: e11814.
[31] Elkamhawy A, Lu Q, Nada H, Woo J, Quan G and Lee K. The journey of DDR1 and DDR2 kinase inhibitors as rising stars in the fight against cancer. Int J Mol Sci 2021; 22: 6535.
[32] Xie X, Rui W, He W, Shao Y, Sun F, Zhou W, Wu Y and Zhu Y. Discoidin domain receptor 1 activity drives an aggressive phenotype in bladder cancer. Am J Transl Res 2017; 9: 2500-2507.
[33] Yang JC, Zhang Y, He SJ, Li MM, Cai XL, Wang H, Xu LM and Cao J. TM4SF1 promotes metastasis of pancreatic cancer via regulating the expression of DDR1. Sci Rep 2017; 7: 45895.
[34] Rudra-Ganguly N, Lowe C, Mattie M, Chang MS, Satpayev D, Verlinsky A, An Z, Hu L, Yang P, Challita-Eid P, Stover DR and Pereira DS. Discoidin domain receptor 1 contributes to tumorigenesis through modulation of TGFBI expression. PLoS One 2014; 9: e111515.
[35] Chiusa M, Hu W, Liao HJ, Su Y, Borza CM, de Caestecker MP, Skrypnyk NI, Fogo AB, Pedchenko V, Li X, Zhang MZ, Hudson BG, Basak T, Vanacore RM, Zent R and Pozzi A. The extracellular matrix receptor discoidin domain receptor 1 regulates collagen transcription by translocating to the nucleus. J Am Soc Nephrol 2019; 30: 1605-1624.
[36] Shintani Y, Fukumoto Y, Chaika N, Svoboda R, Wheelock MJ and Johnson KR. Collagen I-mediated up-regulation of N-cadherin requires cooperative signals from integrins and discoidin domain receptor 1. J Cell Biol 2008; 180: 1277-1289.
[37] Bouchard V, Harnois C, Demers MJ, Thibodeau S, Laquerre V, Gauthier R, Vézina A, Noël D, Fujita N, Tsuruo T, Arguin M and Vachon PH. B1 integrin/Fak/Src signaling in intestinal epithelial crypt cell survival: integration of complex regulatory mechanisms. Apoptosis 2008; 13: 531-42.